

EXPLORING NEW FEATURES OF NEUTRINO OSCILLATIONS WITH A TRITON SOURCE AND A LARGE SPHERICAL TPC

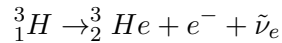
Y. Giomataris¹ and J.D. Vergados²

1 CEA, Saclay, DAPNIA, Gif-sur-Yvette, Cedex, France

2 University of Ioannina, Ioannina, GR 45110, Greece
E-mail: Vergados@cc.uoi.gr

Abstract

The purpose of the present paper is to study the neutrino oscillations as they may appear in the low energy neutrinos emitted in triton decay:



with maximum neutrino energy of 18.6 *KeV*. Such low energy neutrino oscillations can only be detected via neutrino electron scattering. The novel feature is the fact that the cross section is sensitive to both charged and neutral currents. Thus one can simultaneously probe the electron neutrino disappearance as well as the appearance of the other two flavors. By folding the differential cross section with the neutrino spectrum one can study the dependence of the oscillation parameters as a function of the electron energy. The technical challenges to this end can be summarized as building a very large TPC capable of detecting low energy recoils, down to a few 100 eV, within the required low background constraints have been previously described [1]. We only mention here that the oscillation length involving the small angle $s_{13} = \sin\theta_{13}$, directly measured in this experiment, is fully contained inside the detector. A sensitivity of a few percent for the measurement of the above angle will be achieved.

Key words: PACS numbers:13.15.+g, 14.60Lm, 14.60Bq, 23.40.-s, 95.55.Vj, 12.15.-y.

1 Introduction.

The discover of neutrino oscillations can be considered as one of the greatest triumphs of modern physics. It began with atmospheric neutrino oscillations [2] interpreted as $\nu_\mu \rightarrow \nu_\tau$ oscillations, as well as ν_e disappearance in solar neutrinos [3]. These results have been recently confirmed by the KamLAND experiment [4], which exhibits evidence for reactor antineutrino disappearance. As a result of these experiments we have a pretty good idea of the neutrino mixing matrix and the two independent quantities Δm^2 , e.g $m_2^2 - m_1^2$ and $m_3^2 - m_2^2$. Fortunately these two Δm^2 are vastly different

$$\Delta m^2(21)m_{21}^2 = |m_2^2 - m_1^2| = (5.0 - 7.5) \times 10^{-5}(eV)^2$$

and

$$\Delta m_{32}^2 = |m_3^2 - m_2^2| = 2.5 \times 10^{-3}(eV)^2.$$

This means that the associated oscillation lengths are very different and the experimental results can effectively be described as two generation oscillations. This has been followed by an avalanche of interesting three generation analyses [5]-[9].

In all of these analyses the oscillation length is much larger than the size of the detector. So one is able to see the effect, if the detector is placed in the right distance from the source. It is, however, possible to design an experiment with an oscillation length of the order of the size of the detector. In this case one can start with zero oscillation near the source, proceed to maximum oscillation near the middle of the detector and end up again with no oscillation on the other end. This is achieved, if one considers a neutrino source with the lowest possible average neutrino energy such as a triton source with a maximum energy of 18.6 keV. Thus the average oscillation length is 6.5m, which is smaller than the radius of 10m of a spherical TPC detector (for a description of the apparatus see our earlier work [1]).

Since the neutrino energies are so small, the only possible detec-

tor sensitive to oscillations is one, which is capable of detecting electrons. With this detector can detect:

- electrons which are produced by electron neutrinos via the charged current interaction, which are depleted by **electron neutrino disappearance**
- electrons which may arise from the other two neutrino flavors due to the neutral current interaction. These two flavors are produced by the **muon and tau neutrino appearance, which operates simultaneously.**

Since these two mechanisms are competing with each other and the subsequent electron cross section depends on the electron energy, one has a novel feature, i.e. the dependence of the effective oscillation probability on the electron energy. Thus the results may appear as disappearance oscillation in some kinematical regime and as appearance oscillation in some other regime. In this paper we will examine how these features can best be exploited in determining the neutrino oscillation parameters.

2 Elastic Neutrino Electron Scattering

For low energy neutrinos the historic process neutrino-electron scattering [10] [11] is very useful. The differential cross section [12] takes the form

$$\frac{d\sigma}{dT} = \left(\frac{d\sigma}{dT}\right)_{weak} + \left(\frac{d\sigma}{dT}\right)_{EM} \quad (2.1)$$

The cross section due to weak interaction alone becomes:

$$\begin{aligned} \left(\frac{d\sigma}{dT}\right)_{weak} &= \frac{G_F^2 m_e}{2\pi} [(g_V + g_A)^2 \\ &+ (g_V - g_A)^2 \left[1 - \frac{T}{E_\nu}\right]^2 + (g_A^2 - g_V^2) \frac{m_e T}{E_\nu^2}] \end{aligned} \quad (2.2)$$

$$g_V = 2 \sin^2 \theta_W + 1/2 \quad (\nu_e), \quad g_V = 2 \sin^2 \theta_W - 1/2 \quad (\nu_\mu, \nu_\tau)$$

$$g_A = 1/2 \quad (\nu_e) \quad , \quad g_A = -1/2 \quad (\nu_\mu, \nu_\tau)$$

For antineutrinos $g_A \rightarrow -g_A$. To set the scale

$$\frac{G_F^2 m_e}{2\pi} = 4.45 \times 10^{-48} \frac{cm^2}{keV} \quad (2.3)$$

The electron energy depends on the neutrino energy and the scattering angle and is given by:

$$T = \frac{2 m_e (E_\nu \cos \theta)^2}{(m_e + E_\nu)^2 - (E_\nu \cos \theta)^2}$$

The last equation can be simplified as follows:

$$T \approx \frac{2(E_\nu \cos \theta)^2}{m_e} \Rightarrow$$

The maximum electron energy depends on the neutrino energy. For $E_\nu = 18.6 \text{ KeV}$ one finds that the maximum electron kinetic energy is:

$$T_{max} \approx 1.27 \text{ KeV}$$

In what follows, whenever appropriate, we are going to average our results with the neutrino spectrum shown in Fig. 2.1.

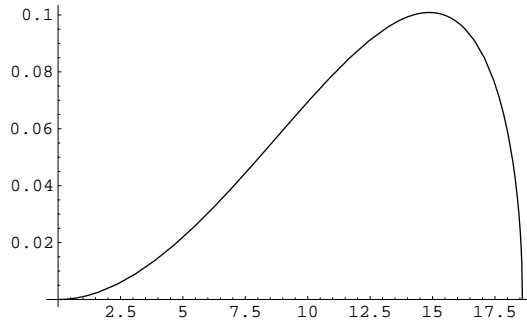


Fig. 2.1. The neutrino spectrum distribution function for the triton source (normalized to unity).

3 NEUTRINO OSCILLATIONS IN THE NOSTOS EXPERIMENT

The electron neutrino is given [1] by:

$$\nu_e = \frac{c \nu_1 + s \nu_2 + s_{13} \nu_3}{1 + s_{13}}$$

where $s \approx \sin\theta_{solar}$, $c \approx \cos\theta_{solar}$, θ_{solar} determined from the solar neutrino data, and $s_{13} = \sin\theta_{13}$ is a small quantity constrained by the CHOOZE experiment to be small. The electron disappearance oscillation probability is given by:

$$P(\nu_e \rightarrow \nu_e) = 1 - 4 \frac{s^2 c^2 \sin^2(\pi \frac{L}{L_{21}}) + \left(s^2 \sin^2(\pi \frac{L}{L_{31}}) + c^2 \sin^2(\pi \frac{L}{L_{32}}) \right) s_{13}^2}{(1 + s_{13}^2)^2}$$

Assuming $\Delta m_{31}^2 \approx \Delta m_{32}^2$ we find:

$$P(\nu_e \rightarrow \nu_e) \approx 1 - \frac{(\sin 2\theta_{solar})^2 \sin^2(\pi \frac{L}{L_{21}}) + 4s_{13}^2 \sin^2(\pi \frac{L}{L_{32}})}{(1 + s_{13}^2)^2}$$

where the term proportional to s_{13}^2 is relevant for NOSTOS ($L_{21} = 50L_{32}$). The NOSTOS experiment, in addition to the electronic neutrinos, which are depleted by the oscillations, is sensitive to the other two neutrino flavors, which can also scatter electrons via the neutral current interactions. These flavors are generated via the appearance oscillation:

$$P(\nu_e \rightarrow \sum_{\alpha \neq e} \nu_\alpha) \approx \frac{(\sin 2\theta_{solar})^2 \sin^2(\pi \frac{L}{L_{21}}) + 4s_{13}^2 \sin^2(\pi \frac{L}{L_{32}})}{(1 + s_{13}^2)^2}$$

Thus the number of the scattered electrons, which bear this rather unusual oscillation pattern, is proportional to the (ν_e, e^-) scattering cross section with a proportionality constant given by:

$$P(\nu_e \rightarrow \nu_e) \approx 1 - \chi(E_\nu, T) \frac{(\sin 2\theta_{solar})^2 \sin^2(\pi \frac{L}{L_{21}}) + 4s_{13}^2 \sin^2(\pi \frac{L}{L_{32}})}{(1 + s_{13}^2)^2} \quad (3.4)$$

where $\chi(E_\nu, T)$ is one minus the fraction of the cross section of flavor ν_μ or ν_τ divided by that of ν_e , i.e.

$$\chi(E_\nu, T) = 4\sin^2\theta_w [2E_\nu^2 - 4TE_\nu + T(2T - m_e)] / [E_\nu^2(1 + 4\sin^2\theta_W + 8\sin^4\theta_W) - 2E_\nu T(1 + 2\sin^2\theta_W)^2 + (1 + 2\sin^2\theta_W)T(2(T - m_e)\sin^2\theta_W + T)] \quad (3.5)$$

The function $\chi(E_\nu, T)$ in the region:

$$E_\nu + \frac{m_e}{4} - \frac{1}{4}\sqrt{8m_e E_\nu + m_e^2} \leq T \leq E_\nu + \frac{m_e}{4} + \frac{1}{4}\sqrt{8m_e E_\nu + m_e^2}$$

becomes negative. This means that the cross section due to ν_μ or ν_τ becomes larger than that of ν_e . This can also be seen by plotting the relevant cross sections, see Figs 3.2 and 3.3. We see that the cross section due to flavor ν_μ or ν_τ is rising, while the one due to ν_e is dropping, see Fig. 3.3. This means that the

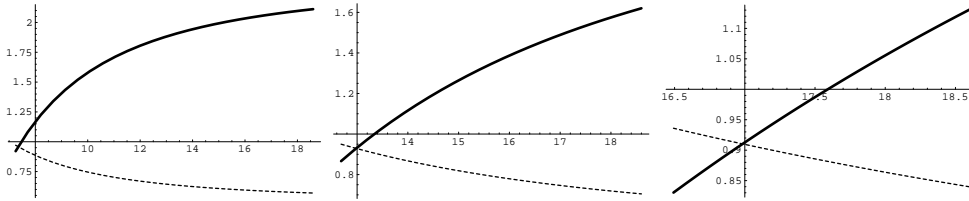


Fig. 3.2. The differential cross (ν_e, e^-) section, in arbitrary units, as a function of the neutrino energy for electron energies from left to right 0.2, 0.6 and 1.0 keV. The the dashed curve corresponds to the cross section due to ν_α , $\alpha = \mu$ or τ .

function $\chi(E_\nu, T)$ eventually changes sign, see Fig. 3.4. If this occurs in a kinematically interesting region, it will lead to neutrino oscillation results different than those naively expected.

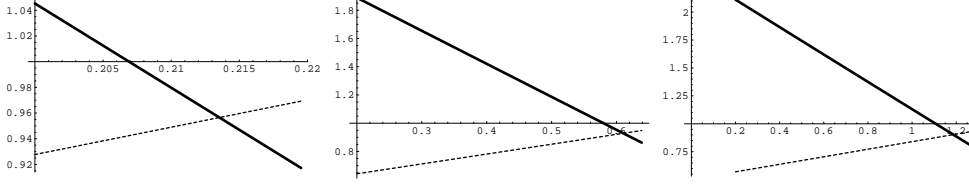


Fig. 3.3. The differential cross (ν_e, e^-) section , in arbitrary units, as a function of the electron energy for neutrino energies from left to right 7.6, 13.1 and 18.6 keV. The the dashed curve corresponds to to the cross section due to ν_α , $\alpha = \mu$ or τ .

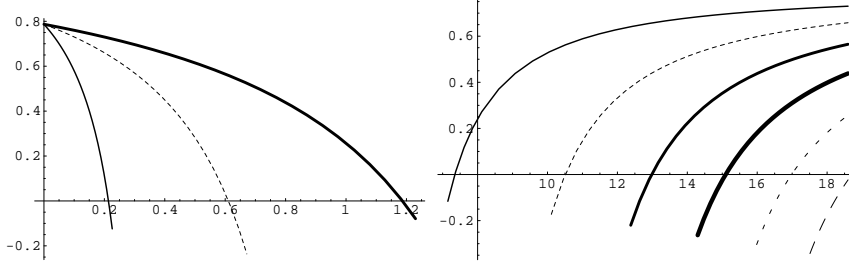


Fig. 3.4. On left the function $\chi(E\nu, T)$ is shown as a function of the electron energy for neutrino energies 7.6 keV (thin line), 13.1 keV (dashed line) and 18.6 KeV (thick line). On the right we show the same quantity as a of the neutrino energy for electron energies 0.2, 0.4, 0.6, 0.8, 1.0, 1.2 keV increasing to the right.

4 VARIOUS PATTERNS OF OSCILLATION PROBABILITIES

The oscillation probabilities for NOSTOS, i.e. near the source, as well as experiments further from the source for $\sin^2 2\theta_{13} = 0.17$ with and without the function $\chi(E_\nu, T)$ are shown in Figs 4.5-4.8. For $\sin^2 2\theta_{13} = 0.085$ in Figs 4.9-4.12 and for $\sin^2 2\theta_{13} = 0.045$ in Figs 4.13-4.16

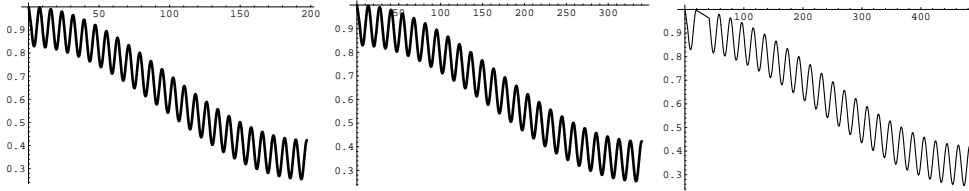


Fig. 4.5. The oscillation probability at distances larger than the NOSTOS size without the function $\chi(E_\nu, T)$. One can see the oscillation associated with Δm_{12}^2 . If sensitive to to $\sin^2 2\theta_{13} = 0.17$ one will also see on top of this the small oscillation associated with Δm_{32}^2 . From left to right, $E_\nu = 7.6, 13.1$ and 18.6 keV.

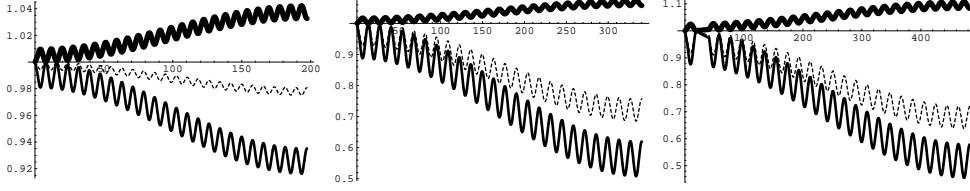


Fig. 4.6. The same as in Fig. 4.5 after including the function $\chi(E_\nu, T)$. The results now depend on the electron energy. For $E_\nu = 7.6$ (left) we show the results for $T = 0.200, 0.213$ and 0.220 keV indicated by thin, dashed and thick line respectively. For $E_\nu = 13.1$ (middle), $T = 0.200, 0.419$ and 0.639 keV, while for $E_\nu = 18.6$ (right), $T = 0.200, 0.731$ and 1.262 keV.

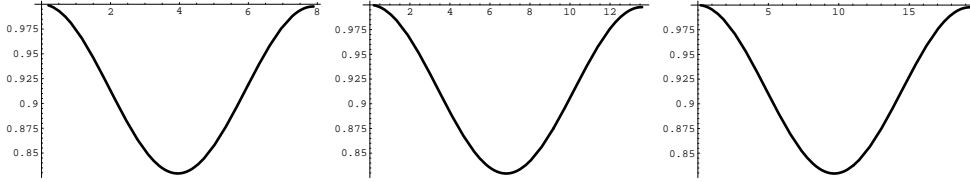


Fig. 4.7. The oscillation probability expected in NOSTOS with $\sin^2 2\theta_{13} = 0.17$ corresponding to, from left to right, $E_\nu = 7.6, 13.1$ and 18.6 keV, without the function $\chi(E_\nu, T)$.

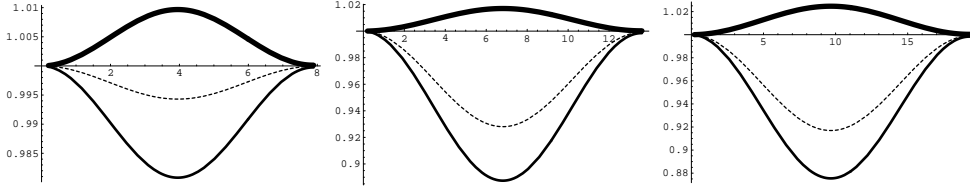


Fig. 4.8. The same as in Fig. 4.7 after including the function $\chi(E_\nu, T)$ and the neutrino and electron energies as indicated in Fig 4.6.

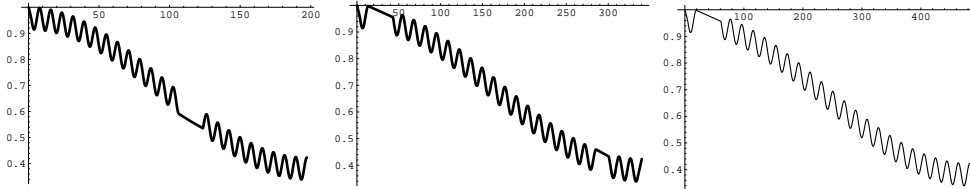


Fig. 4.9. The same as in Fig. 4.5 with $\sin^2 2\theta_{13} = 0.085$.

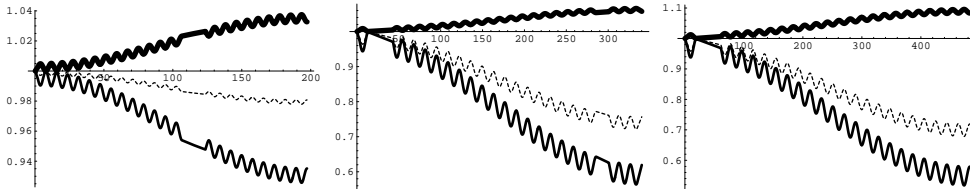


Fig. 4.10. The same as in Fig. 4.6 with $\sin^2 2\theta_{13} = 0.085$.

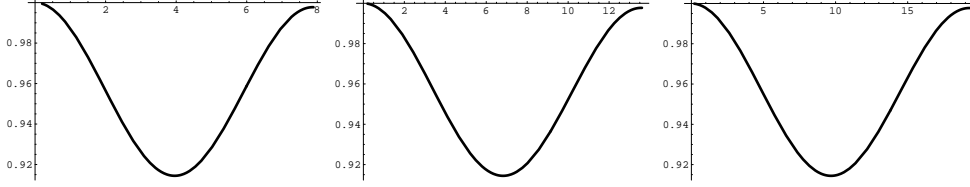


Fig. 4.11. The same as in Fig. 4.7 with $\sin^2 2\theta_{13} = 0.085$.

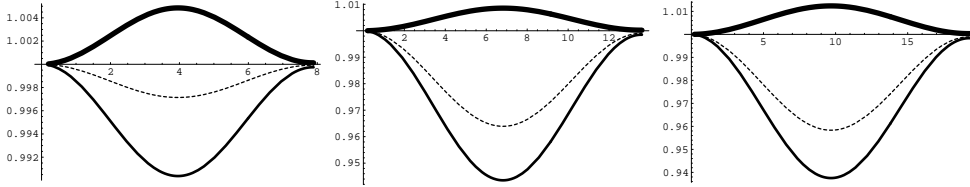


Fig. 4.12. The same as in Fig. 4.8 with $\sin^2 2\theta_{13} = 0.085$.

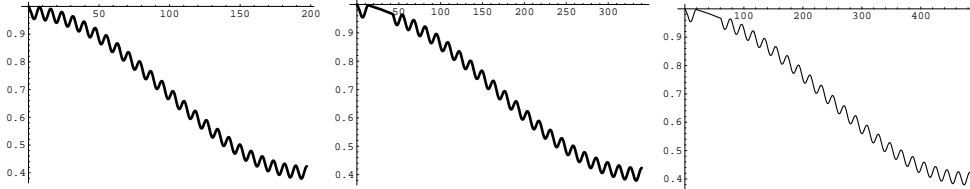


Fig. 4.13. The same as in Fig. 4.5 with $\sin^2 2\theta_{13} = 0.045$.

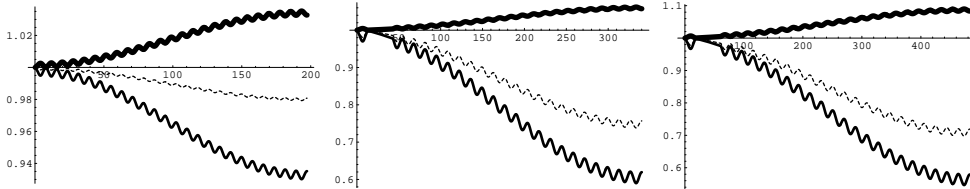


Fig. 4.14. The same as in Fig. 4.6 with $\sin^2 2\theta_{13} = 0.045$.

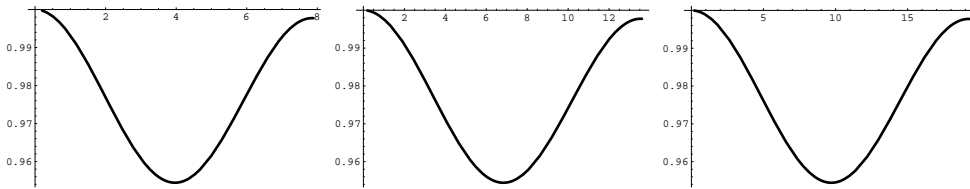


Fig. 4.15. The same as in Fig. 4.7 with $\sin^2 2\theta_{13} = 0.045$.

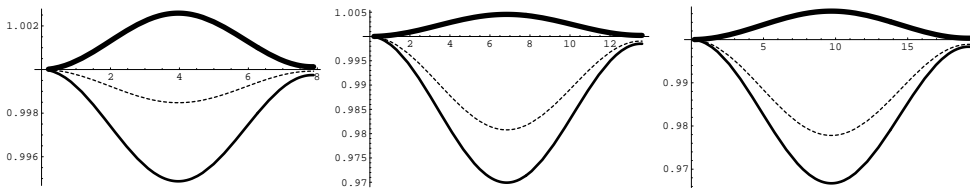


Fig. 4.16. The same as in Fig. 4.8 with $\sin^2 2\theta_{13} = 0.045$.

5 AVERAGED NEUTRINO OSCILLATION PROBABILITIES

With the above ingredients one can obtain an effective neutrino oscillation probability for various electron energies by averaging the expression of the oscillation probability, Eq. (3.4), over the weak differential cross section, Eq. 2.3, and the neutrino spectrum, see Fig. 2.1, i.e.

$$\langle P(\nu_e \rightarrow \nu_e) \rangle = \frac{\int P(\nu_e \rightarrow \nu_e) \left(\frac{d\sigma}{dT}\right)_{weak} f_\nu(E_\nu) dE_\nu}{\int \left(\frac{d\sigma}{dT}\right)_{weak} f_\nu(E_\nu) dE_\nu} \quad (5.6)$$

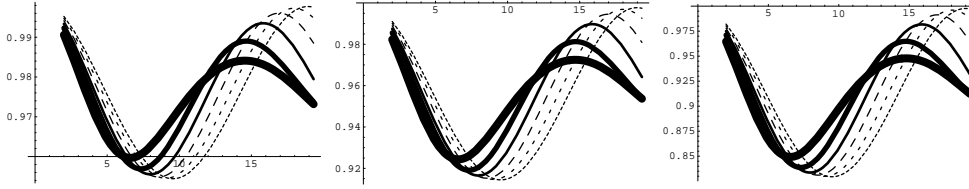


Fig. 5.17. The average oscillation probability as a function of the radial distance L (in meters). We have integrated over the neutrino spectrum, but the function $\chi(E_\nu, T)$ was not included. From left to right $\sin^2 2\theta_{13} = 0.045, 0.085, 0.170$. The depth is increasing with T

Oscillations for $\sin^2 2\theta_{13} = 0.17$ as seen in distances far greater than the NOSTOS experiment as well as in the NOSTOS experiment are shown in Figs 4.5-4.8 both with and without the function $\chi(E_\nu, T)$. Results for $\sin^2 2\theta_{13} = 0.085, 0.045$ are shown in Figs 4.9-4.12 and 4.13-4.16 respectively.

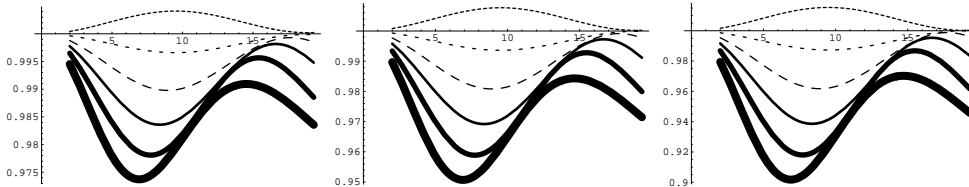


Fig. 5.18. The average oscillation probability as a function of the radial distance L . We have integrated over the neutrino spectrum and included the function $\chi(E_\nu, T)$. From left to right $\sin^2 2\theta_{13} = 0.045, 0.085, 0.170$. Labeling as in Fig. 5.17.

6 RESULTS

We now are going to present what the NOSTOS experiment is going to measure, namely the differential cross section averaged over the neutrino spectrum, i.e.

$$\begin{aligned} \langle \frac{d\sigma}{dT} \rangle &= \int P(\nu_e \rightarrow \nu_e) \left(\frac{d\sigma}{dT} \right)_{weak} f_\nu(E_\nu) dE_\nu \\ &= \langle P(\nu_e \rightarrow \nu_e) \rangle \langle f_e(T) \rangle \end{aligned} \quad (6.7)$$

Or

$$\langle \frac{d\sigma}{dT} \rangle = \langle P(\nu_e \rightarrow \nu_e) \rangle \langle f_e(T) \rangle \quad (6.8)$$

$$\langle f_e(T) \rangle = \int \left(\frac{d\sigma}{dT} \right)_{weak} f_\nu(E_\nu) dE_\nu \quad (6.9)$$

The results obtained are shown in Figs 6.19-6.20. We see that, unfortunately, the unexpected oscillation features are washed out. They stood out mainly due to the fact that we normalized the amplitude in the usual way, i.e. so that the oscillation length independent part of the amplitude is equal to unity. They happen, however, to occur in a kinematically unfavored region, where the cross sections is small. Indeed the differential cross section, averaged over the neutrino spectrum, as we have seen can also be obtained by multiplying the average oscillation probability with the function given by Eq. 6.9 (see Eqs 6.8 and 5.6). The latter quantity is shown in Fig. 6.22. We thus see that the contribution of the high energy electrons becomes very small. One can, of course, obtain the total cross section by integrating the differential cross section over the electron energy as a function of the distance from the source. The thus obtained results are shown in Fig. 6.23.

Experimentally, of course, one measures events. The number of events is obtained by:

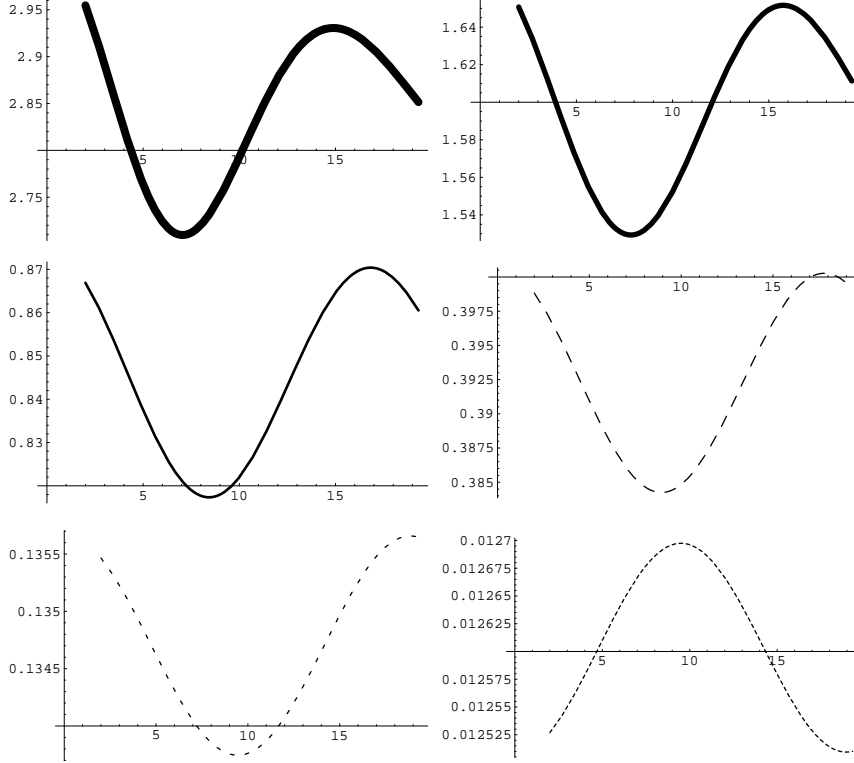


Fig. 6.19. The differential cross (ν_e, e^-) section, $\langle \frac{d\sigma}{dT} \rangle$, in units of $\frac{G_F^2 m_e}{2\pi} = 4.5 \times 10^{-52} \frac{m^2}{keV}$, as a function of the source-detector distance averaged over the neutrino energy for electron energies from top to bottom and left to right 0.2, 0.4, 0.6, 0.8, 1.0 and 1.2 keV. The results shown correspond to $\sin^2 2\theta_{13} = 0.170$

- Inserting in the relevant cross sections the scale of weak interaction

$$\frac{G_F^2 m_e}{2\pi} = 4.50 \times 10^{-52} \frac{m^2}{keV}$$

- Considering the total number of neutrinos emitted by the source of 20 Kg of tritium

$$N_\nu = \frac{20}{3 \times 1.67 \times 10^{-27}} = 4.00 \times 10^{27}$$

for any given time t the number of neutrinos emitted must be multiplied by the fraction $1 - e^{-t/\tau}$ with $\tau = \frac{T_{1/2}}{\ln 2} \simeq 17.7y$ ($T_{1/2} = 12.3y$). This yields the neutrino flux:

$$\Phi_\nu = \frac{N_\nu}{4\pi L^2} (e^{-t/\tau} / \tau)$$

- Assuming that in the target the number of electrons per unit

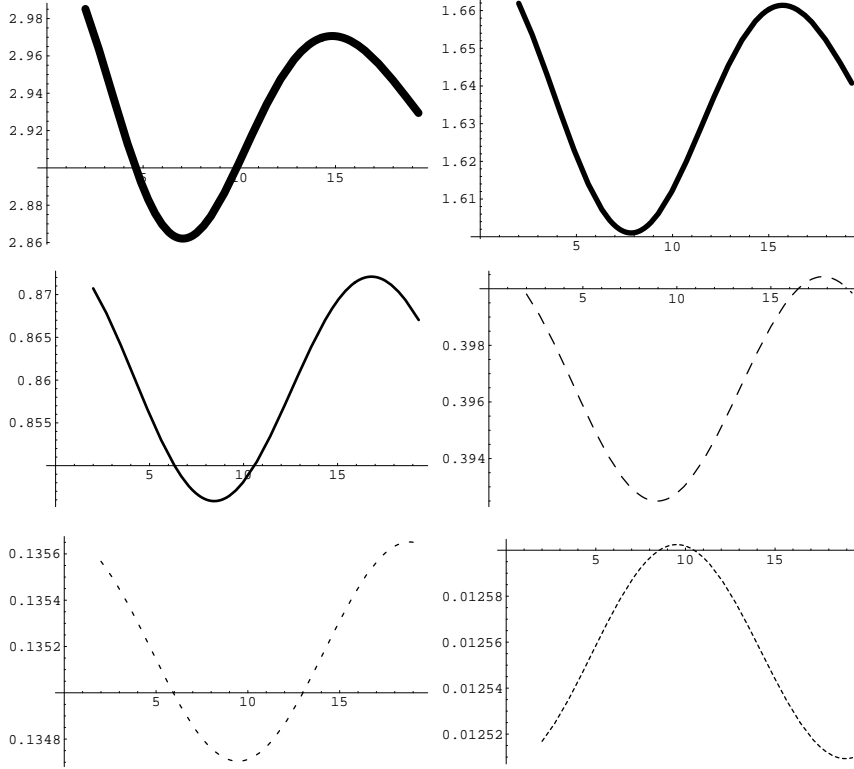


Fig. 6.20. The same as in Fig. 6.19 for $\sin^2 2\theta_{13} = 0.085$
volume is

$$n_e = Z \frac{P}{kT_0} = 4.4 \times 10^{27} m^{-3} \frac{P}{10 \text{ Atm}} \frac{Z}{18} \frac{300}{T_0}$$

(Z the atomic number, P is the pressure and T_0 the temperature).

- The total number of events with energies between T and $T + dT$ in the length region between L and $L + dL$ is

$$dN = \Phi_\nu \frac{d\sigma}{dT} n_e 4\pi L^2 dT dL = N_\nu \frac{d\sigma}{dT} n_e dT dL.$$

For any given time t we get only the fraction $1 - e^{-t/\tau}$ of these events, e.g 5% the first year, 11% for two years of running, 16% after 3 years and 43% after 10 years.

The thus obtained results for the differential rate $\frac{dN}{dT dL}$, during the life time of the source (20 Kg of tritium), employing $^{40}_{18}\text{Ar}$ at $P = 10 \text{ Atm}$, are shown in Fig. 6.24-6.26. The total rate per unit length, obtained by integrating the differential rate of Fig.

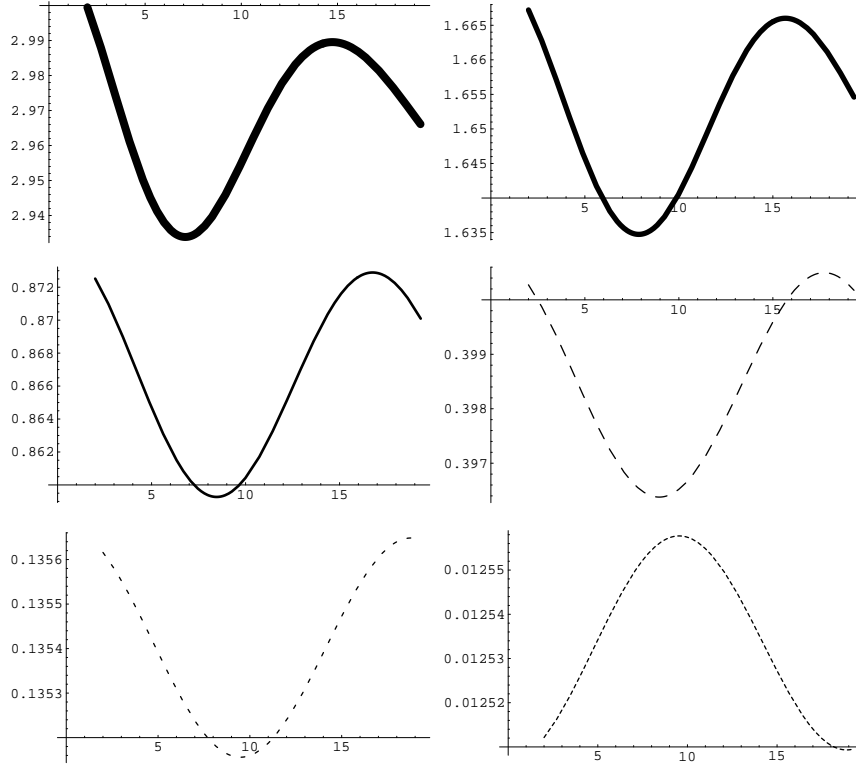


Fig. 6.21. The same as in Fig. 6.19 for $\sin^2 2\theta_{13} = 0.045$

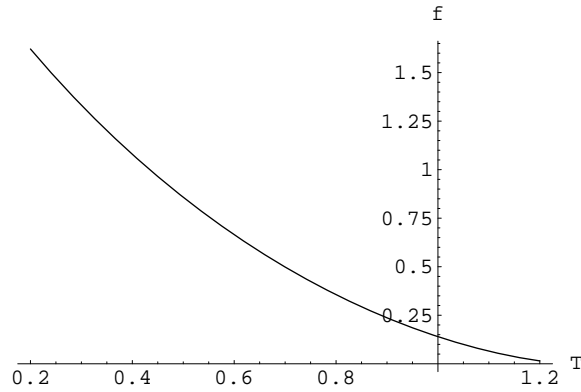


Fig. 6.22. $\langle f_e(T) \rangle$, the differential cross (ν_e, e^-) section without oscillations, in units of $\frac{G_F^2 m_e}{2\pi} = 4.5 \times 10^{-52} \frac{m^2}{keV}$, averaged over the neutrino spectrum, as a function of the outgoing electron energy in keV.

6.24-6.26 with respect to the electron energy, is shown in Fig. 6.27.

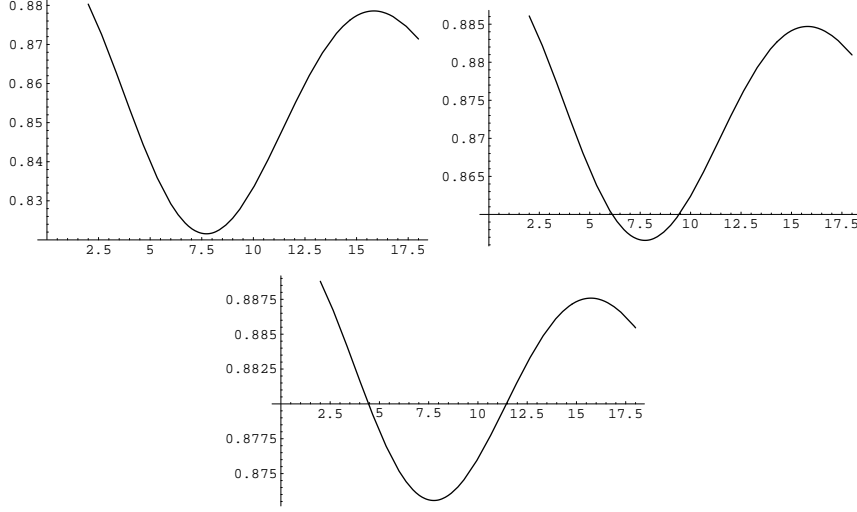


Fig. 6.23. The total cross section, in units of $\frac{G_F^2 m_e}{2\pi} = 4.5 \times 10^{-52} \text{cm}^2$, as a function of the source detector distance. From top to bottom and left to right for $\sin^2 2\theta_{13} = 0.170, 0.85, 0.045$.

7 Discussion and Conclusions

In the experiment one will measure the differential rate, i.e. the number of electrons detected per unit energy and per unit length, as a function of the distance L from the source, i.e. the radius of the sphere. Integrating the differential rate one obtains the number of electrons per unit length as a function of L . From Figs 6.24-6.26 and 6.27, obtained with a source of 20 Kg of tritium over its lifetime and using Ar at 10 Atm, we see that the L -dependence of the event rates resembles closely that of the corresponding cross sections shown in Figs 6.19-6.21 and 6.23. To get the event rate after some time t of running, we must multiply by the factor $1 - e^{-t/\tau}$, $\tau = 17.7\text{y}$, e.g. 5% during the first year etc. The event rates scale with the atomic number Z . From these plots we see that:

- In the case of the differential rate:
 - (1) At high electron energies it increases as a function of L , i.e. it behaves like appearance oscillation. The electrons are mainly produced by the other two appearing neutrino flavors. This is a novel feature of the neutrino electron scattering.
 - (2) At low electron energies, where the cross section is large, one

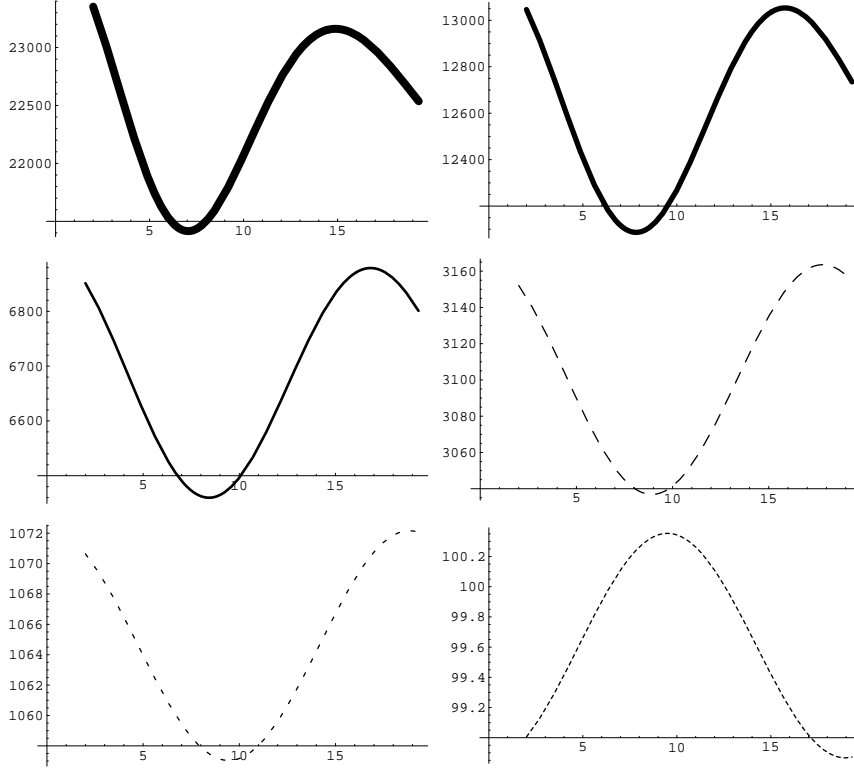


Fig. 6.24. The differential rate $\frac{dN}{dT dL}$ (per keV-meter) for Ar at 10 Atm with 20 Kg of tritium as a function of the source-detector distance (in m), averaged over the neutrino energy, for electron energies from top to bottom and left to right 0.2, 0.4, 0.6, 0.8, 1.0 and 1.2 keV. The results shown correspond to $\sin^2 2\theta_{13} = 0.170$. This rate must be multiplied by $1 - e^{-t/\tau}$ to get the number of events after running time t . Thus only 5% of these are expected during the first year of running.

recovers the usual features of electron flavor disappearance.

- (3) The difference between the maximum and the minimum is at the level of 8, 4 and 2 % for $\sin^2 2\theta_{13} = 0.170$, 0.085 and 0.045 respectively.
- (4) The location of the maximum depends on the electron energy.
 - In the case of the total cross section:
 - (1) The percentage of the difference between the maximum and the minimum is about the same as before.
 - (2) The maximum of the oscillation probability occurs at $L = 7.5$ m.

It is clear that with such a large number of events the above features of neutrino oscillation can be exploited to measure $\sin^2 2\theta_{13}$ and perhaps to accurately determine the oscillation length.

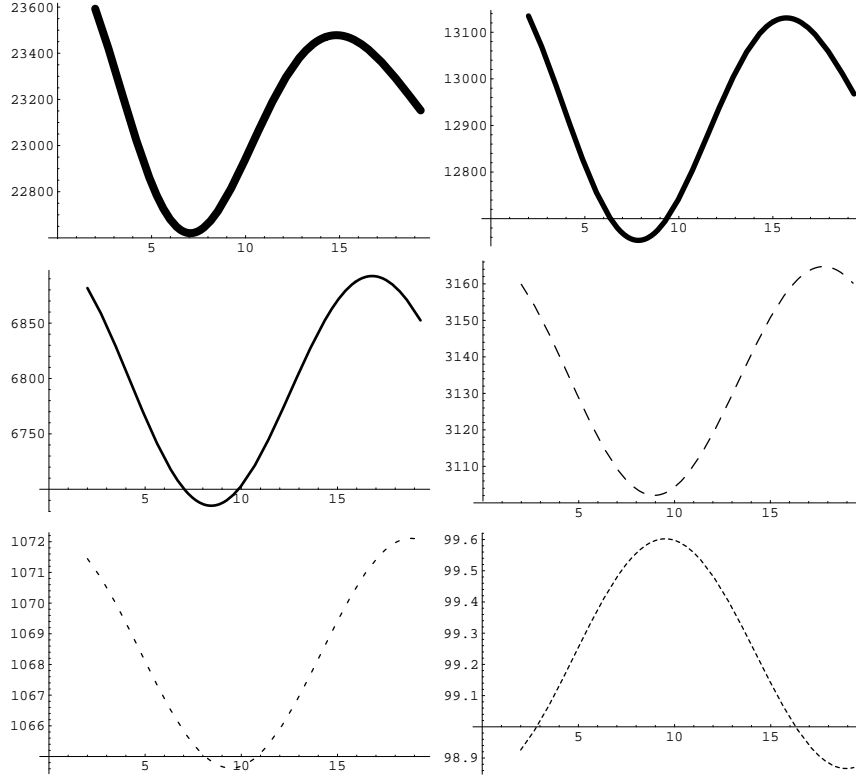


Fig. 6.25. The same as in Fig. 6.24 for $\sin^2 2\theta_{13} = 0.085$.

acknowledgments: This work was supported in part by the European Union under the contract MRTN-CT-2004-503369 and by the program PYTHAGORAS-1 of the Operational Program for Education and Initial Vocational Training of the Hellenic Ministry of Education under the 3rd Community Support Framework and the European Social Fund.

References

- [1] Y. Giomataris and J.D. Vergados, *Nucl. Instr. Meth. A* **53** (2004) 330.
- [2] Y. Fukuda *et al*, The Super-Kamiokande Collaboration, *Phys. Rev. Lett.* **86**, (2001) 5651; *ibid* **81** (1998) 1562 & 1158; *ibid* **82** (1999) 1810 ;*ibid* **85** (2000) 3999.
- [3] Q.R. Ahmad *et al*, The SNO Collaboration, *Phys. Rev. Lett.* **89** (2002) 011302; *ibid* **89** (2002) 011301 ; *ibid* **87** (2001) 071301.
 K. Lande *et al*, Homestake Collaboration, *Astrophys. J* **496**, (1998) 505
 W. Hampel *et al*, The Gallex Collaboration, *Phys. Lett. B* **447**, (1999) 127;
 J.N. Abdurashitov *al*, Sage Collaboration, *Phys. Rev. C* **80** (1999) 056801;
 G.L Fogli *et al*, *Phys. Rev. D* **66** (2002) 053010.

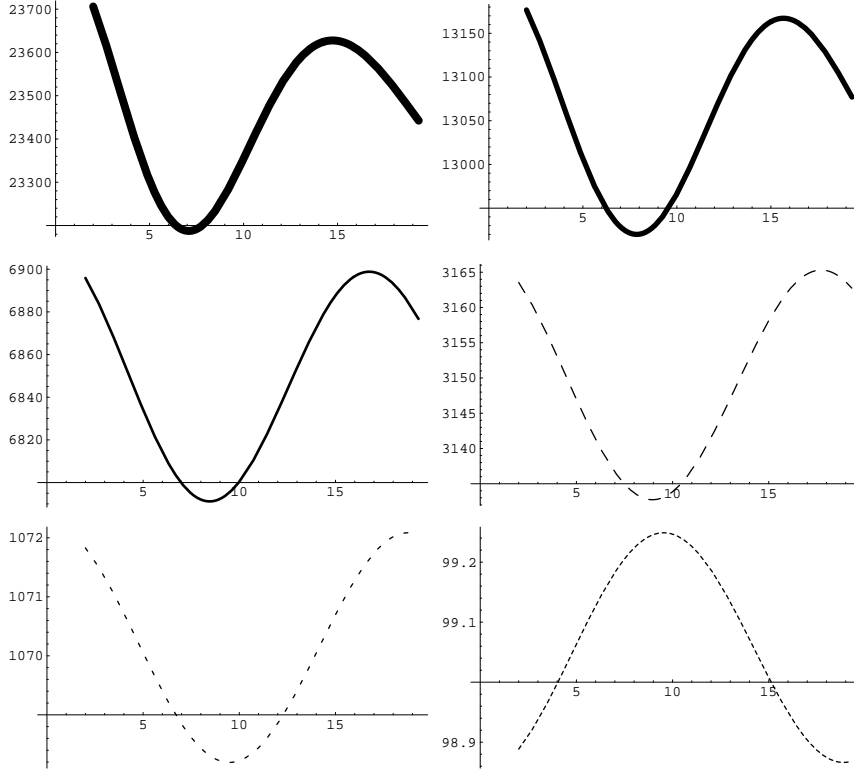


Fig. 6.26. The same as in Fig. 6.24 for $\sin^2 2\theta_{13} = 0.045$.

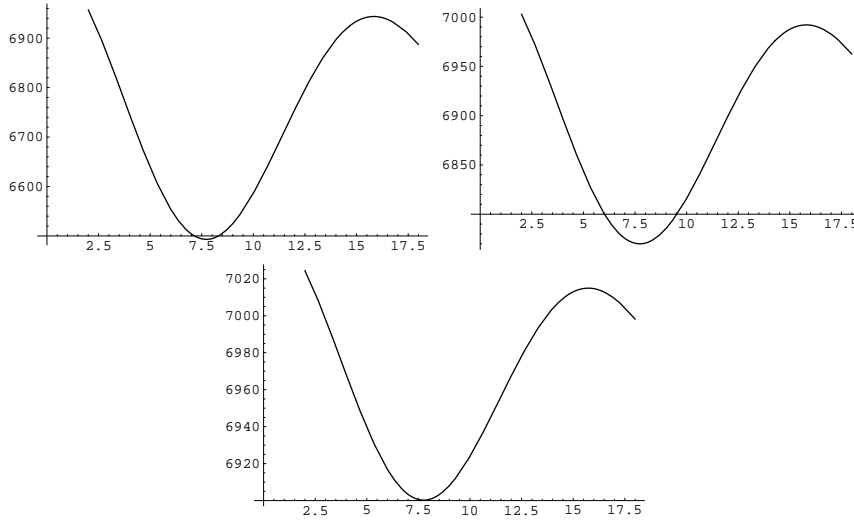


Fig. 6.27. The total event rate as a function of the source detector distance. The notation is the same as in Fig. 6.23. The input is the same as in Fig. 6.24.

[4] K. Eguchi *et al*, The KamLAND Collaboration, *Phys. Rev. Lett.* 90 (2003) 021802, hep-exp/0212021.

[5] J,N. Bahcall, M.C. Gonzalez-Garcia, C. Peña-Garay, *hep-ph/0212147*

[6] H Nunokawa *et al*, *hep-ph/0212202*.

- [7] P. Aliani *et al*, *hep-ph/0212212*.
- [8] M. Maltoni, T. Schwetz and J.F. Valle, *hep-ph/0212129*; S. Pakvasa and J.F. Valle, *hep-ph/0301061*
- [9] V. Barger and D. Marfatia, *hep-ph/0212126*.
- [10] G. 't Hooft, *Phys. Lett. B* **37** (1971) 195.
- [11] F. Reines, H.S. Gurr and H.W. Sobel, *Phys. Rev. Lett.* **6** (1976) 315.
- [12] P. Vogel and J. Engel, *Phys. Rev. D* **39** (1989) 3378.